R-Site Substitution Effect on the Oxygen-Storage Capability of $RBaCo_4O_{7+\delta}$

S. Kadota,[†] M. Karppinen,*[,†,‡] T. Motohashi,[†] and H. Yamauchi[†,‡]

Materials and Structures Laboratory, Tokyo Institute of Technology, Yokohama 226-8503, Japan, and Laboratory of Inorganic Chemistry, Department of Chemistry, Helsinki University of Technology, FI-02015 TKK, Finland

Received May 23, 2008. Revised Manuscript Received August 9, 2008

Here we show that the low-temperature oxygen-storage capability of $RBaCo_4O_{7+\delta}$ (R = Y, Dy, Ho, Er, Tm, Yb, and Lu) depends on the size of the rare earth constituent R. For all these R constituents the $RBaCo_4O_{7+\delta}$ phase can be charged and discharged with large amounts of oxygen in a narrow temperature range below 400 °C. With decreasing ionic radius, $r(R^{III})$, the oxygen-release temperature (T_R) decreases while the temperature where the phase decomposes (T_D) increases such that the "safety window" between T_R and T_D widens. On the other hand, the maximum amount of excess oxygen taken by the $RBaCo_4O_{7+\delta}$ lattice in 1 atm O_2 decreases from $\delta \approx 1.4$ (for R = Dy) to ~1.0 (for R = Lu) with decreasing $r(R^{III})$. Hence the optimum oxygen-storage characteristics are found about R = Tm in terms of $r(R^{III})$. We also discuss the crystal structures of the oxygen-annealed $RBaCo_4O_{7+\delta}$ samples.

Introduction

The layered cobalt oxide, $YBaCo_4O_{7+\delta}$, has been revealed to possess unique low-temperature oxygen absorption/desorption characteristics.[1,2] Through normal-pressure oxygen annealing, it is possible to charge the phase with excess oxygen up to $\delta \approx 1.4$ and then discharge it back to $\delta \approx 0.0$ within a narrow temperature range of 200−400 °C where the oxygen absorption/desorption process is sensitively controlled by just tiny changes in temperature and/or oxygen partial pressure. The oxygen-storage capacity (OSC; capacity for reversible uptake and release of oxygen) of $YBaCo_4O_{7+\delta}$ (OSC ≈ 2450 μmol-O/g) substantially exceeds the values reported for conventional oxygen-storage materials, e.g., CeO_2-ZrO_2 (OSC ≈ 1500 μmol-O/g).[3,4] Through high-pressure annealing, even larger amounts of oxygen ($\delta \approx 1.56$[5] or OSC ≈ 2700 μmol-O/g) could be loaded in $YBaCo_4O_{7+\delta}$. Moreover, compared to the traditional materials the operation temperature range where the reversible charging and discharging cycle is possible is appreciably low in $YBaCo_4O_{7+\delta}$. Applications readily imaginable for $YBaCo_4O_{7+\delta}$ range from gas-separation membranes to solid-oxide fuel cells as well as oxygen sensors. The material might also find a number of uses as a relatively mild source of reactive oxygen for various chemical and biological processes. Moreover, it is a highly relevant candidate for an efficient oxygen-gas separator for perfect separation between H_2 and O_2 gases; such a separator is urgently demanded to make the photocatalytic decomposition of water by sunlight feasible.

Even though the basic crystal structure of the oxygen-poor form of $YBaCo_4O_{7+\delta}$ ($\delta = 0$) was determined already in 2002,[6] much less is known about the crystal structure(s) of the oxygenated phase(s). The parent $YBaCo_4O_7$ structure is of hexagonal symmetry (space group $P6_3mc$[6] or $P31c$[7]) and consists of two kinds of corner-sharing CoO_4 tetrahedra (with a ratio of 1:3) located in separate, alternately stacked layers of triangular and Kagomé types. Recently Chmaissem et al.[8] described in a satisfactory manner the crystal structure of their $YBaCo_4O_{8.1}$ sample in orthorhombic space group $Pbc2_1$ on the basis of high-resolution neutron and synchrotron X-ray powder diffraction data. In their structure model Co atoms occupy both corner-sharing tetrahedral and edge-sharing octahedral sites. Whether the most strongly oxygenated $YBaCo_4O_{7+\delta}$ samples (up to $\delta \approx 1.56$[5]) should be described with the same/related structure has not been fully addressed yet.[9] In fact, even with a full occupation of all the oxygen sites available in the $Pbc2_1$ structure, the maximum amount of oxygen described by it remains at $\delta = 1.0$.

As for potential applications, one would yet like to improve certain material properties of $YBaCo_4O_{7+\delta}$. One of the most serious disadvantages of $YBaCo_4O_{7+\delta}$ may be the thermo-

* Corresponding author: Laboratory of Inorganic Chemistry, Department of Chemistry, Helsinki University of Technology, P.O. Box 6100, FI-02015 TKK, Finland. Fax: +358-9-462373. Tel.: +358-9-451-2600. E-mail: maarit.karppinen@tkk.fi.

† Tokyo Institute of Technology.

‡ Helsinki University of Technology.

(1) Karppinen, M.; Yamauchi, H.; Otani, S.; Fujita, T.; Motohashi, T.; Huang, Y. H.; Valkeapää, M.; Fjellvåg, H. *Chem. Mater.* **2006**, *18*, 490.

(2) Karppinen, M.; Yamauchi, H.; Fjellvåg, H.; Motohashi, T. Int. Patent Appl., PCT/JP2006313436, filed June 6, 2006.

(3) Nagai, Y.; Yamamoto, T.; Tanaka, T.; Yoshida, S.; Nonaka, T.; Okamoto, T.; Suda, A.; Sugiura, M. *Catal. Today* **2002**, *74*, 225.

(4) Motohashi, T.; Kadota, S.; Fjellvåg, H.; Karppinen, M.; Yamauchi, H. *Mater. Sci. Eng., B* **2008**, *148*, 196.

(5) Räsänen, S.; Yamauchi, H.; Karppinen, M. *Chem. Lett.* **2008**, *37*, 638.

(6) Valldor, M.; Andersson, M. *Solid State Sci.* **2002**, *4*, 923.

(7) Huq, A.; Mitchell, J. F.; Zheng, H.; Chapon, L. C.; Radaelli, P. G.; Knight, K. S.; Stephens, P. W. *J. Solid State Chem.* **2006**, *179*, 1136.

(8) Chmaissem, O.; Zheng, H.; Huq, A.; Stephens, P. W.; Mitchell, J. F. *J. Solid State Chem.* **2008**, *181*, 664.

(9) Valkeapää, M.; Karppinen, M.; Motohashi, T.; Liu, R. S.; Chen, J. M.; Yamauchi, H. *Chem. Lett.* **2007**, *36*, 1368.

10.1021/cm801412q CCC: $40.75
Published on Web 09/18/2008

dynamical instability at low temperatures relative to the more highly oxidized $BaCoO_{3-\delta}$ phase. Actually, $YBaCo_4O_{7+\delta}$ is thermodynamically stable only at high temperatures, in air at temperatures higher than ~900 °C.[1] However, once the phase is successfully synthesized at a high temperature (and preferably at a low oxygen partial pressure), it remains kinetically stabilized as a metastable phase at low temperatures and as aforementioned even withstands the low-temperature (200−400 °C) oxygen charging/discharging without any degradation. Only when being heated in an oxygen-containing atmosphere beyond ~600 °C does $YBaCo_4O_{7+\delta}$ decompose into $BaCoO_{3-\delta}$. Here an effort should be made to increase the decomposition temperature (T_D) and, if possible, simultaneously decrease the temperature (T_R) at which the phase releases the excess oxygen upon heating to make the "safety window", $T_R \sim T_D$, wider.

There indeed are a number of possible approaches toward further optimization of the $YBaCo_4O_{7+\delta}$ phase based on the fact that it readily accepts various cation substitutions. For instance, yttrium may be fully replaced by any of the other small rare earth elements (R = Dy ~ Lu) without affecting the basic $YBaCo_4O_7$ structure.[10] Here we demonstrate that the smaller-for-larger R^{III}-cation substitution works for widening the $T_R \sim T_D$ window. Moreover, discussed is the open question concerning the crystal structure(s) of the oxygenated phase(s) of $YBaCo_4O_{7+\delta}$ and its $RBaCo_4O_{7+\delta}$ derivatives.

Experimental Section

High-quality samples of $RBaCo_4O_{7+\delta}$ (R = Y, Dy, Ho, Er, Tm, Yb, and Lu) were synthesized through a wet-chemical route[11] using R_2O_3 (fired at 850 °C overnight prior to use), $Ba(NO_3)_2$, and $Co(NO_3)_2 \cdot 6H_2O$ as starting materials. Stoichiometric amounts of these powders were dissolved in a concentrated HNO_3 solution in which ethylene-diaminetetraacetic acid (EDTA)/NH_3 solution was subsequently added to bind the metal ions. After the EDTA addition, the solution was dried and burned into raw ash, which was then pelletized and sintered at 1050 °C (1075 °C for R = Lu) in N_2 gas flow. After a 20 h sintering period, the samples were furnace-cooled to room temperature without cutting out the N_2 gas flow.

The as-synthesized $RBaCo_4O_{7+\delta}$ samples (with $\delta \approx 0.1$) were characterized for their oxygen absorption/desorption and thermal decomposition behaviors by means of thermogravimetric (TG; Rigaku TG8120) measurements carried out for ~20 mg specimens in O_2 gas flow (200 mL/min) up to 1000 °C. In these measurements the heating rate was kept slow (1 °C/min) with an anticipation that the TG curves would at every datum point represent a state close to thermodynamic equilibrium. Moreover, from each as-synthesized sample a specimen of ~100 mg was separated and then annealed in O_2 gas flow at 260 °C to reach the maximum oxygen content. These annealing experiments were carried out in a thermobalance as well (heating rate = 10 °C/min; isothermal keeping period = 24 h; cooling rate = 20 °C/min). Additionally, one sample with an intermediate oxygen content ($\delta = 1.08$ according to subsequent oxygen-content analysis) was prepared for R = Y by annealing a specimen of the as-synthesized sample in O_2 gas flow at 320 °C for 24 h (in a thermobalance). Here the goal was to synthesize a sample as close as possible to the one characterized by Chmaissem et al.[9] ($\delta \approx 1.1$) for the precise crystal structure.

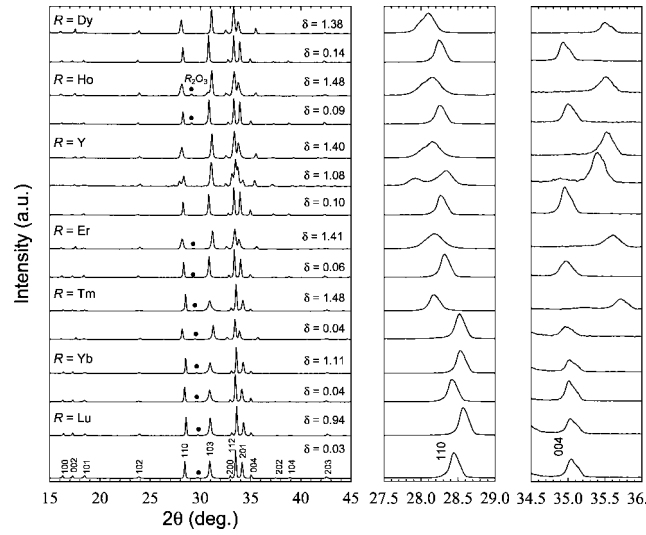

Figure 1. XRD patterns for the as-synthesized and oxygenated samples of $RBaCo_4O_{7+\delta}$. The indices given in the bottom pattern for the $LuBaCo_4O_{7.03}$ sample are based on space group $P6_3mc$. The right-hand side panels magnify the 2θ ranges for the 110 and the 004 reflections.

Table 1. Oxygen Contents of the Present $RBaCo_4O_{7+\delta}$ Samples

	oxygen content δ		
R	as-N_2-synthesized	fully oxygenated: O_2, 260 °C, 24 h	partly oxygenated: O_2, 320 °C, 24 h
Dy	0.14	1.38	
Ho	0.09	1.48	
Y	0.10	1.40	1.08
Er	0.06	1.41	
Tm	0.04	1.48	
Yb	0.04	1.11	
Lu	0.03	0.94	

Phase purity and lattice parameters were checked for all the as-synthesized and oxygen-annealed samples by X-ray powder diffraction (XRD; Rigaku RINT-2500V equipped with a Cu rotating anode; JANA2000 software). Oxygen contents were determined for the samples by means of iodometric titration.[12] For the titration experiment, the sample was dissolved in 1 M HCl solution containing an excess of KI as the reductant. Then, titration of the resultant I_2 was performed with 0.005 M $Na_2S_2O_3$ solution using starch as an indicator. For each sample, the analysis was repeated seven times to reveal the oxygen content with a reproducibility of ±0.01.

Results and Discussion

Judging from the XRD data (see Figure 1), the present $RBaCo_4O_{7+\delta}$ samples were all essentially single phase: the only impurity peaks seen for some of the samples are due to trace amounts of unreacted R_2O_3. For all the as-synthesized samples iodometric titration yielded oxygen-content values of $\delta \approx 0.1$ (see Table 1). For these samples the diffraction patterns were readily indexed according to the hexagonal space group $P6_3mc$ originally reported for $YBaCo_4O_7$.[6] This is demonstrated for the R = Lu case in Figure 1.

Thermal behaviors of the as-synthesized samples were investigated in O_2 gas flow by means of thermogravimetric measurements carried out with a slow heating rate of 1 °C/min up to 1000 °C. The resultant TG curves are displayed

(10) Valldor, M. *Solid State Sci.* **2004**, *6*, 251.
(11) Huang, Y. H.; Lindén, J.; Yamauchi, H.; Karppinen, M. *Chem. Mater.* **2004**, *16*, 4337.
(12) Karppinen, M.; Matvejeff, M.; Salomäki, K.; Yamauchi, H. *J. Mater. Chem.* **2002**, *12*, 1761.

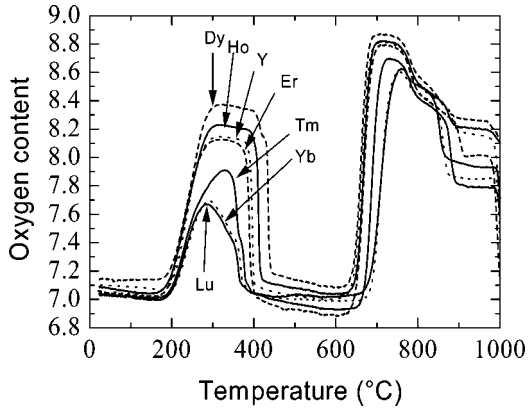

Figure 2. TG curves for as-synthesized $RBaCo_4O_{7+\delta}$ samples ($0.03 \leq \delta \leq 0.14$) recorded in O_2 gas flow with a heating rate of 1 °C/min. The two humps at about 200−400 °C and above 600 °C are due to oxygen absorption/desorption and phase decomposition, respectively.

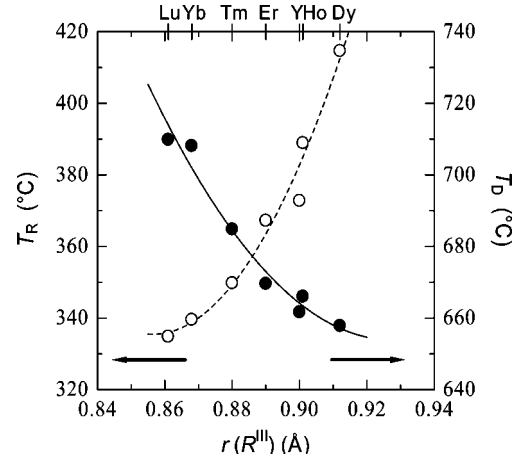

Figure 3. Oxygen-reduction (T_R; ○) and phase-decomposition (T_D; ●) temperatures plotted for the $RBaCo_4O_{7+\delta}$ system against the ionic radius, $r(R^{III})$ of the rare earth constituent, R (= Y, Dy, Ho, Er, Tm, Yb, and Lu).

in Figure 2. For each $RBaCo_4O_{7+\delta}$ sample, the TG curve exhibits two humps. The hump in the lower temperature region of 200−400 °C reflects the unique ability of the $RBaCo_4O_{7+\delta}$ compounds to absorb and then desorb large amounts of oxygen in a narrow temperature range, whereas the one in the high-temperature region above 600 °C is due to the phase decomposition of $RBaCo_4O_{7+\delta}$ to $BaCoO_{3-\delta}$.[1] From Figure 2, it is obvious that both the phenomena are affected by the choice of the rare earth species R. First, the shapes of the curves regarding the low-temperature hump (due to oxygen intake and release) are different for different R's. For the smallest R's (=Lu and Yb) the oxygen release process occurs in two clearly distinguishable steps, whereas for the larger R's a kind of plateau is seen before the start of the oxygen release which occurs in an essentially single abrupt step. Second, the maximum amount of excess oxygen loaded in the $RBaCo_4O_{7+\delta}$ lattice during the TG run clearly depends on the species of R, increasing with increasing size of R. Third, both the oxygen-release temperature T_R and the temperature T_D where the decomposition starts depend on R in a systematic manner. In the following these three observed features are discussed in reverse order.

From Figure 2, both T_R and T_D depend on R such that T_R decreases and T_D increases with decreasing size of the R constituent. To clarify this situation in a more quantitative way, we plot in Figure 3 T_R's and T_D's for all the $RBaCo_4O_{7+\delta}$ phases against the ionic radius of the R constituent, $r(R^{III})$. Note that the values of T_R the T_D were taken from the corresponding TG derivative curves (DTG: $\Delta m/\Delta T$; not shown here) at the maximum points in the temperature regions related to the oxygen release and the phase decomposition, respectively. From Figure 3, throughout the R-substitution range studied, T_R systematically decreases (by ∼80 °C) and T_D increases (by ∼50 °C) with decreasing $r(R^{III})$. Hence we may conclude that for the $RBaCo_4O_{7+\delta}$ system decreasing the size of the R constituent widens by more than 100 °C the temperature window $T_R \sim T_D$, which provides the tolerance for the material to be safely employed for oxygen storage or other related functions/applications.

According to the TG curves presented in Figure 2, the maximum level of excess oxygen reachable during a dynamical TG run (with a heating rate of 1 °C/min) decreases with decreasing $r(R^{III})$. To confirm whether the same trend is seen for the real equilibrium oxygen-content values of the different $RBaCo_4O_{7+\delta}$ phases, isothermal (24 h) O_2 annealing experiments were carried out for all the as-synthesized samples at 260 °C (to maximize the oxygen content) and additionally at 320 °C for R = Y to obtain a $YBaCo_4O_{7+\delta}$ sample with an intermediate oxygen content. The resultant oxygen-content values (from iodometric titration) are summarized in Table 1. For the smallest R constituents, the maximum oxygen contents achieved in 1 atm O_2, i.e., $\delta =$ 0.94 for Lu and 1.11 for Yb, are significantly lower than those for the rest of the R's for all of which the maximum oxygen contents were $\delta \approx 1.4$.

From Figure 2 also revealed was that the shape of the TG curve in the oxygen absorption/desorption region of 200−400 °C depends on R. Most importantly, it is clear that the oxygen desorption occurs differently for different $RBaCo_4O_{7+\delta}$ phases, that is, in two easily distinguishable steps (with different mass loss versus temperature rates) for the smaller *R* samples and in an essentially single step for the larger R samples. Even though it is not possible to end up with any concrete conclusion based on the present XRD data (collected with a laboratory diffractometer), it is tempting to relate the different oxygen-release behaviors to small but definite differences in the crystal structure of the fully oxygenated $RBaCo_4O_{7+\delta}$ samples, e.g., different sites and/or different bonding strengths for the excess oxygen atoms. From Figure 1, with display of the XRD patterns for all the as-synthesized and oxygen-annealed samples, several observations can be made. Common to all the phases, though more significant for the larger R's, is that upon oxygen loading the peaks get somewhat broader. (Here it should be noted that the peak broadening is not due to changes in particle size. This possibility was ruled out by careful SEM analysis, which revealed that the particle size of our $RBaCo_4O_{7+\delta}$ samples remains constantly at ∼2 μm upon oxygen charging and discharging.) Another general observation is that the peaks overall shifted to higher 2θ angles upon oxygen loading, which apparently reflects the fact that the $RBaCo_4O_{7+\delta}$ lattice shrinks due to an increase in the oxidation state of cobalt.[1,5,9]

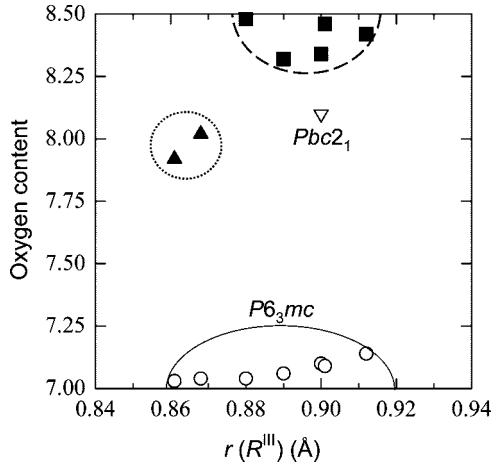

Figure 4. Phase diagram for oxygen content versus ionic radius $r(R^{III})$ in the $RBaCo_4O_{7+\delta}$ system (R = Y, Dy, Ho, Er, Tm, Yb, and Lu). The phase diagram involves at least four different crystal structures. Space groups for the data with open symbols (○ and ▽) are as indicated. Those for the data with solid symbols (■ and ▲) are not determined yet.

However, the diffraction-peak shifts are not exactly parallel for all the samples with different R's; see the two right-hand-side panels of Figure 1. For R = Dy, Ho, Y, Er, and Tm, the 002 and 004 peaks (according to space group $P6_3mc$ that explains the oxygen-poor $RBaCo_4O_7$ crystal structure) are shifted toward the higher angle side but the 110 peak just to the opposite direction, whereas for R = Yb and Lu the 002 and 004 peaks remain unchanged but the 110 peak is shifted toward the higher angle side. The diffraction pattern for the R = Y sample with $\delta = 1.08$ could be readily fitted with the orthorhombic space group $Pbc2_1$ (revealed by Chmaissem et al.[8] for their $\delta \approx 1.1$ sample), but the space group did not work for any of the fully oxygenated $RBaCo_4O_{7+\delta}$ samples. Moreover, it is clear that the diffraction patterns for the fully oxygenated R = Lu and Yb samples differ from those of the other fully oxygenated samples (with R = Dy, Ho, Y, Er, and Tm). The situation is summarized in Figure 4 to demonstrate that in the $RBaCo_4O_{7+\delta}$ system the crystal structure is not defined only by the amount of excess oxygen δ, but it also depends on $r(R^{III})$ as the two samples, $LuBaCo_4O_{7.94}$ and $YbBaCo_4O_{8.11}$ (with the smallest R constituents), have a different structure from that of the $YBaCo_4O_{8.08}$ sample (with $Pbc2_1$). Finally, we should emphasize that for all the $RBaCo_4O_{7+\delta}$ phases it was confirmed that the diffraction patterns (not shown here) for samples annealed in a thermobalance in O_2 gas flow up to 500 °C and then quenched to room temperature were identical to those for the corresponding as-synthesized samples. In other words, after the oxygen charging/discharging cycle the crystal structure indeed returns to the original $RBaCo_4O_7$ ($P6_3mc$) structure, as expected.

Conclusion

In the present work we have demonstrated that the rather unique low-temperature oxygen-storage characteristics of $RBaCo_4O_{7+\delta}$ depend on the size of the rare earth constituent R. Upon decreasing of the ionic radius $r(R^{III})$, the oxygen-release temperature T_R decreases while the phase-decomposition temperature T_D increases such that the "safety window", $T_R \sim T_D$, widens. However, at the same time the maximum amount of excess oxygen chargeable into the $RBaCo_4O_{7+\delta}$ lattice in 1 atm O_2 decreases as the size of R becomes smaller. Hence, the oxygen-storage characteristics for the $RBaCo_4O_{7+\delta}$ system may be optimized about R = Tm.

The present work has also suggested that the mechanism behind the oxygen absorption/desorption phenomenon might depend on the detailed crystal structure of the phases in the $RBaCo_4O_{7+\delta}$ system that overall includes at least four distinguishable crystal structures depending on δ and $r(R^{III})$. Here we emphasize the importance of efforts to determine all these different crystal structures by state-of-the art diffraction techniques for full understanding of the oxygen absorption/release mechanism in $RBaCo_4O_{7+\delta}$.

Acknowledgment. This work was supported by a Grant for R & D of New Interdisciplinary Fields in Nanotechnology and Materials Program of MEXT of Japan and also by Tekes (No. 1726/31/07) and Academy of Finland (Nos. 110433 and 116254).

CM801412Q